Systematic microcanonical analyses of polymer adsorption transitions

Monika Möddel,[a] Wolfhard Janke[b] and Michael Bachmann[c]

In detailed microcanonical analyses of densities of states obtained by extensive multicanonical Monte Carlo computer simulations, we investigate the caloric properties of conformational transitions that adsorbing polymers experience near attractive substrates. For short chains and strong surface attraction, the microcanonical entropy turns out to be a convex function of energy in the transition regime, indicating that surface-entropic effects are relevant. Albeit known to be a continuous transition in the thermodynamic limit of infinitely long chains, the adsorption transition of nongrafted finite-length polymers thus exhibits a clear signature of a first-order-like transition, with coexisting phases of adsorbed and desorbed conformations. Another remarkable consequence of the convexity of the microcanonical entropy is that the transition is accompanied by a decrease of the microcanonical temperature with increasing energy. Since this is a characteristic physical effect it might not be ignored in analyses of cooperative macrostate transitions in finite systems.

1 Introduction

The advances in processing and manipulating molecules at solid substrates on the nanometre scale opens up new vistas for technological applications of hybrid organic-inorganic interfaces. This includes, *e.g.*, the fabrication of nanostructured transistors being sensitive to specific biomolecules[1,2] and the application of organic electronic devices based on polymers such as organic light-emitting diodes[3] and molecular storage cells.[4] Therefore, the investigation of molecular self-assembly[5,6] near substrates has recently been the subject of numerous experimental and computational studies, *e.g.*, for peptide adhesion to metals and semiconductors.[7–13] The understanding of the cooperative effects of structure formation at substrates requires systematic studies of mesoscopic aspects of adsorption transitions. This includes scaling properties near the adsorption/desorption transition in the thermodynamic limit of large polymer systems at planar surfaces,[14–17] also under pulling force.[18,19] Adhesion studies of polymers were also performed at curved surfaces such as nanotubes[20] and nanoparticles.[21] Particular attention has been dedicated to the complete phase structure of adsorbed macromolecules which has been investigated by means of simple lattice models for polymers[22–27] and peptides,[28,29] as well as by employing an off-lattice polymer model.[30]

Hybrid systems on the nanoscopic scale must basically be considered as being "small". Thus, the study of finite-size effects in the formation of polymer assemblies in a thermal environment is relevant. Here, we are going to discuss thermodynamic properties of the adsorption transition of a flexible, interacting polymer at an attractive substrate. The polymer is not anchored at the surface and can therefore freely move as long as it does not get into contact with the substrate. Statistical analysis is performed in the microcanonical ensemble in order to retain characteristic, non-negligible surface effects. This approach has already proven quite useful for a deeper understanding of first-order-like structural transitions such as molecular aggregation processes[31,32] and protein folding.[33,34]

A particularly striking result was the recent identification of intrinsic hierarchies of subphase transitions that accompany the overall cooperative process of assembly.[32] The relevance of microcanonical thermodynamics[35] in small-system transitions has also been stated in simulational and experimental atomic clustering studies,[36,37] fragmenting nuclei,[38] and for scaling analyses in magnetic systems employing discrete or continuous spin models.[39–43] A more exotic example is the seminal application of this approach to astrophysical systems,[44] which manifests its broad universality.

The central quantity in the microcanonical formalism is the number (or density) of states $g(E)$ with system energy E, or the microcanonical entropy defined as

$$S(E) = k_B \ln g(E), \tag{1}$$

where k_B is the Boltzmann constant. In contrast to canonical (NVT) statistics, where the temperature T is an externally fixed control parameter, in the microcanonical (NVE) ensemble it is *derived* from the entropy,

$$T(E) = [\partial S(E)/\partial E]_{N,V}^{-1}. \tag{2}$$

In both ensembles, the particle number N and the volume V are kept fixed. Particularly interesting microcanonical effects occur in the transition regime, if the entropy is a convex function of energy in this region. The physical consequence is that with *increasing* system energy the temperature *decreases*. This can only be explained by the fact that conformational transitions of small systems are governed by

[a] *Institut für Theoretische Physik and Centre for Theoretical Sciences (NTZ), Universität Leipzig, Postfach 100 920, D-04009 Leipzig, Germany. E-mail: Monika.Moeddel@itp.uni-leipzig.de*
[b] *Institut für Theoretische Physik and Centre for Theoretical Sciences (NTZ), Universität Leipzig, Postfach 100 920, D-04009 Leipzig, Germany. E-mail: Wolfhard.Janke@itp.uni-leipzig.de*
[c] *Institut für Festkörperforschung (IFF-2) and Institute for Advanced Simulation (IAS-2), Forschungszentrum Jülich, D-52425 Jülich, Germany. E-mail: m.bachmann@fz-juelich.de*

their surfaces, whereas volume effects become only relevant for large systems [even a perfectly icosahedral atomic cluster with 309 atoms still contains more atoms in the outer shell (162) than in the interior (147)].
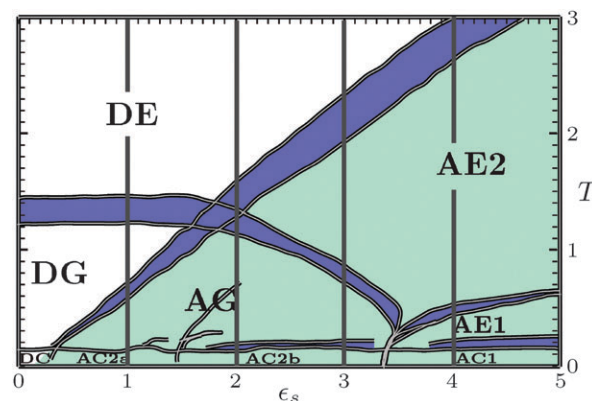
Thus, as long as the surface-to-volume ratio is large enough to suppress a concave increase of the microcanonical entropy and the energetic separation of the two distinct phases [one of which is entropy-dominated (*e.g.*, liquid) and the other energy-dominated (*e.g.*, solid)] is sufficiently large to establish a kinetic barrier, microcanonical effects matter. This regards all first-order phase transitions and two-state systems (*e.g.*, proteins with two-state folding characteristics). It also matters for transitions, where phase co-existence is completely absent in the thermodynamic limit, but not for the finite systems. The latter case is what we would like to consider in more detail in the following: the adsorption transition of flexible polymers to an attractive substrate, known to be a second-order phase transition in the thermodynamic limit. However, as we will show here, the adsorption of nongrafted polymers with finite lengths exhibits signals of a first-order transition which we find to vanish in the thermodynamic limit.

2 Model and methods

For our analysis, we consider a single flexible and nongrafted linear homopolymer with N monomers that interacts with an attractive planar substrate. In ref. 30, we have already employed this hybrid model for the strictly canonical identification of conformational adsorption phases. Here, we concentrate ourselves on the adsorption/desorption transition between desorbed (DE) and three-dimensional adsorbed (AE2) expanded conformations (see Fig. 1), where "three-dimensional" refers to the topology of the dominant adsorbed conformations in AE2, extending into directions parallel and perpendicular to the substrate (in contrast to the preferably planar structures in AE1).

The polymer is represented by a bead-stick model with standard Lennard-Jones (LJ) interaction between nonbonded monomers, mimicking short-range volume exclusion and long-range van der Waals (vdW) attraction. Bond lengths between adjacent monomers are normalized to unity. Since the original model (called the "AB model")[45,46] was designed for mesoscopic heteropolymers, an additional weak bending energy was introduced which is kept here. The only degrees of freedom in our polymer model are thus the angles between successive bonds. Center-of-mass translation is restricted to a cavity bounded by the attractive substrate located at $z = 0$ and a sufficiently distant steric wall at $z = L_z$ to prevent the polymer from escaping. Later in this paper we will discuss the dependence of the microcanonical results on L_z in detail. If not mentioned otherwise, the monomer density is kept constant, *i.e.*, L_z scales linearly with the length of the chain N (we chose $L_z = 3N$, *i.e.*, a constant concentration of monomers). Translation in the xy-plane parallel to the walls is irrelevant here.

The interaction of a monomer with the continuous flat surface of a substrate filling the half-space $z \leq 0$ is obtained by integrating a 12-6-LJ potential over this half-space, which results in a 9-3-LJ-like potential.[30,47] In our simulations, all

Fig. 1 Pseudo-phase diagram of a homopolymer with 20 monomers as obtained in extensive simulations; details are discussed in ref. 30. The bands separate the individual conformational phases, the band width indicates the statistical uncertainty. DE, DG, and DC denote bulk phases of expanded coils, globular, and crystalline structures, respectively. DE and DG are separated by the Θ-transition. AE1 is dominated by adsorbed single-layer (two-dimensional) expanded structures, AE2 by adsorbed conformations extending into the bulk. AG denotes the adsorbed globular regime and the crystalline phases differ in their topology (AC1: two-dimensional, AC2a,b: three-dimensional). In this work, we will primarily focus on the adsorption transition between DE and AE2. Vertical lines are placed at values of surface-attraction strengths ε_s chosen for the subsequent discussion of microcanonical effects accompanying this transition.

lengths are measured in units of the vdW radius $\sigma = 2^{-1/6}r_{\mathrm{min}}$, where r_{min} is the minimum of the 12-6-LJ potential, and energies in units of a global energy scale ε_0. Thus, the temperature scale is given by ε_0/k_B. Accordingly, for simplicity, we set in the following $\sigma = \varepsilon_0 = k_B \equiv 1$. The energy of the hybrid system is then written as:

$$E = 4 \sum_{i=1}^{N-2} \sum_{j=i+2}^{N} (r_{ij}^{-12} - r_{ij}^{-6}) + \frac{1}{4} \sum_{i=1}^{N-2} [1 - \cos(\vartheta_i)]$$
$$+ \varepsilon_s \sum_{i=1}^{N} \left(\frac{2}{15} z_i^{-9} - z_i^{-3} \right),$$

$$(3)$$

where $0 \leq \vartheta_i \leq \pi$ denotes the bending angle between monomers i, $i + 1$, and $i + 2$. The distance between the monomers i and j is $r_{ij} = |\vec{r}_j - \vec{r}_i|$ and z_i is the distance of the ith monomer from the substrate. The free parameter ε_s represents the surface attraction strength and weighs the energy scales of monomer–surface (E_{surf}) and intrinsic monomer–monomer (E_{bulk}) interaction.

In order to improve the sampling of entropically suppressed energetic states, simulations of this model were performed with the multicanonical Monte Carlo method,[48] which is based on a generalized ensemble where the energy histogram is constant and hence directly yields an estimate for the density of states $g(E)$. This can be achieved by Monte Carlo sampling of polymer conformations X with the transition probability

$$\omega(X \to X') = \min[W_{\mathrm{muca}}(E(X'))/W_{\mathrm{muca}}(E(X)), 1], \quad (4)$$

where $W_{\mathrm{muca}}(E(X)) = g^{-1}(E(X))$ is the multicanonical weight function. Since $g(E)$ is obviously unknown in the beginning,

$W_{\text{muca}}(E(X))$ has to be determined recursively. Starting, *e.g.*, with $W_{\text{muca}}^{(0)}(E)$ = const, the energy distribution is almost "flat", if the estimate for the density of states after the nth run, $\hat{g}^{(n)}(E)$, satisfies

$$\hat{g}^{(n)}(E)W_{\text{muca}}^{(n-1)}(E) \approx \text{const.} \qquad (5)$$

An efficient, error-weighted estimation method for $W_{\text{muca}}(E)$ is discussed in ref. 49. The recursion scheme can be stopped if the weight function estimate has stabilized. Then, the density of states $g(E)$ can finally be measured in a long multicanonical production run based on these weights.
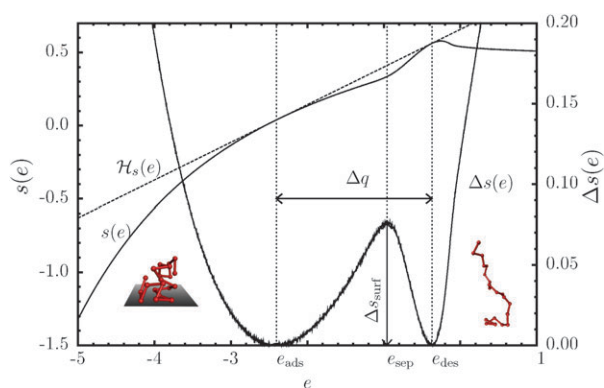
Exemplified for a polymer with 20 monomers and a surface attraction strength $\varepsilon_{\text{s}} = 5$, we have plotted in Fig. 2 the microcanonical entropy per monomer $s(e) = N^{-1}\ln g(e)$ as a function of the energy per monomer $e = E/N$. It shows the characteristic microcanonical features of a transition with phase coexistence in a small system. For energies right below e_{ads}, the system is in the adsorbed phase AE2 (*cf.* Fig. 1), *i.e.*, the polymer is in contact with the substrate, but monomer–monomer contacts are not particularly favored and thus expanded conformations dominate. For energies between e_{ads} and e_{des}, the system is in the transition region, where $s(e)$ is convex. This is clearly seen by constructing the Gibbs hull

$$\mathscr{H}_s(e) = s(e_{\text{ads}}) + e(\partial s/\partial e)_{e = e_{\text{ads}}} \qquad (6)$$

as the tangent that touches $s(e_{\text{ads}})$ and $s(e_{\text{des}})$. Thus,

$$T_{\text{ads}} = \left(\frac{\partial \mathscr{H}_s}{\partial e}\right)^{-1} = \left(\frac{\partial s}{\partial e}\right)^{-1}_{e=e_{\text{ads}}} = \left(\frac{\partial s}{\partial e}\right)^{-1}_{e=e_{\text{des}}} \qquad (7)$$

is the microcanonical *definition* of the adsorption temperature, which coincides with the temperature determined in canonical simulations by the frequently employed criterion of two equal-height peaks in the energy distribution.[40] However, due to the convex well of $s(e)$, the definition of a single transition

Fig. 2 Microcanonical entropy $s(e)$ (up to an unimportant constant) for a 20mer at $\varepsilon_{\text{s}} = 5$, the Gibbs hull $\mathscr{H}_s(e)$, and the difference $\Delta s(e) = \mathscr{H}_s(e) - s(e)$ as functions of the energy per monomer e. The convex adsorption regime is bounded by the energies $e_{\text{ads}} = -2.412$ and $e_{\text{des}} = -0.369$ of the coexisting phases of adsorbed and desorbed conformations at the adsorption temperature $T_{\text{ads}} = 3.885$, as defined *via* the slope of $\mathscr{H}_s(e)$. The maximum of $\Delta s(e)$, called surface entropy Δs_{surf}, is found at $e_{\text{sep}} = -0.962$, which defines the energy of phase separation. The latent heat Δq is defined as the energy being necessary to cross the transition region at the transition temperature T_{ads}.

temperature is misleading; the transition rather spans a region of temperatures. Equivalently, for small systems in the canonical ensemble, fluctuation maxima or two equal-weight peaks are located at different temperatures[50] which also renders the definition of a unique transition temperature impossible. This is obvious for finite systems like proteins, where the thermodynamic limit is unreachable.[51] A unique definition of the transition point is in general only possible in the thermodynamic limit.

Let us define the deviation between $s(e)$ and $\mathscr{H}_s(e)$ by

$$\Delta s(e) = \mathscr{H}_s(e) - s(e). \qquad (8)$$

Then, the surface (or interfacial) entropy, which represents the entropic barrier of the two-state transition, is defined as the maximum deviation

$$\Delta s_{\text{surf}} = \max\{\Delta s(e)|e_{\text{ads}} \leq e \leq e_{\text{des}}\}. \qquad (9)$$

The peak is located at $e = e_{\text{sep}}$ and defines the energetic phase-separation point. Finally, the energetic gap between the two macrostates is the latent heat per monomer,

$$\Delta q = e_{\text{des}} - e_{\text{ads}} = T_{\text{ads}}[s(e_{\text{des}}) - s(e_{\text{ads}})]. \qquad (10)$$

In the thermodynamic limit, a first-order phase transition will be characterized as usual by $\lim_{N \to \infty}\Delta q = \text{const} > 0$, whereas $\lim_{N \to \infty}\Delta q = 0$ in the case of a second-order transition. However, in both cases we expect the surface entropy to vanish in this limit, $\lim_{N \to \infty}\Delta s_{\text{surf}} = 0$, *i.e.*, the microcanonical entropy is always a concave function of energy for infinitely large systems. Before we show for the adsorption transition that the latent heat indeed decreases with system size, we first investigate the origin of the phase separation for chains of finite length and discuss the adhesion strength dependence of surface entropy and microcanonical temperature.
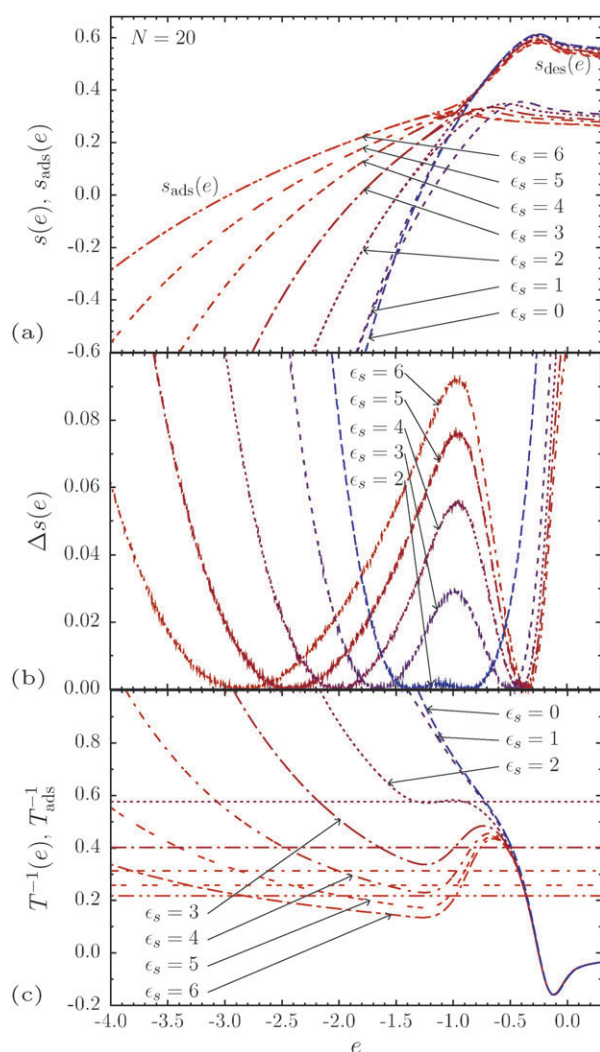
3 Results

3.1 Dependence on the surface attraction strength

In Fig. 3(a), the microcanonical entropy $s(e)$ is shown for a 20mer, parametrized by the surface attraction strength ε_{s}. Since the high-energy regime is dominated by desorbed conformations, the density of states and hence $s(e)$ are hardly affected by changing the values of ε_{s}. The low-energy tail, on the other hand, increases significantly with ε_{s}. Thus, it is useful to split the density of states into the contributions of desorbed and adsorbed conformations, $g_{\text{des}}(e)$ and $g_{\text{ads}}(e)$, respectively, such that $g(e) = g_{\text{des}}(e) + g_{\text{ads}}(e)$ and $s_{\text{des,ads}}(e) = N^{-1}\ln g_{\text{des,ads}}(e)$.

We define the polymer to be adsorbed if its total surface energy is $E_{\text{surf}} < -0.1\varepsilon_{\text{s}}N$. Since $s_{\text{des}}(e)$ corresponds to $s_{\varepsilon_s = 0}(e)$, for $\varepsilon_{\text{s}} > 0$ only the $s_{\text{ads}}(e)$ curves were added in Fig. 3(a). Both, $s_{\text{ads}}(e)$ and $s_{\text{des}}(e)$, are concave in the whole energy range of the adsorption transition. Thus, convex entropic monotony can only occur in the most sensitive region where adsorbed and desorbed conformations have equal entropic weight, *i.e.*, at the entropic transition point. Note that for a polymer *grafted* at the substrate the translational entropy would be very small. The thus far less pronounced increase of $s_{\text{des}}(e)$ at the entropic transition point is not sufficient to induce the convex intruder and no microcanonical peculiarities appear in this case.

Fig. 3 (a) Microcanonical entropies and its fraction for adsorbed conformations $s_{ads}(e)$ at various surface attraction strengths $\varepsilon_s = 0,1,\ldots,6$ for a 20mer [the fraction of desorbed structures corresponds to $s(e)$ for $\varepsilon_s = 0$]; (b) deviations $\Delta s(e)$ from the respective Gibbs hulls (not shown) to illustrate the increase of the surface entropy Δs_{surf} and the latent heat Δq with the attraction strength ε_s. Note that $\Delta s_{surf} = \Delta q = 0$ for $\varepsilon_s = 0,1$; (c) caloric inverse temperature curves $T^{-1}(e)$ and Maxwell lines at respective reciprocal transition temperatures T_{ads}^{-1}.
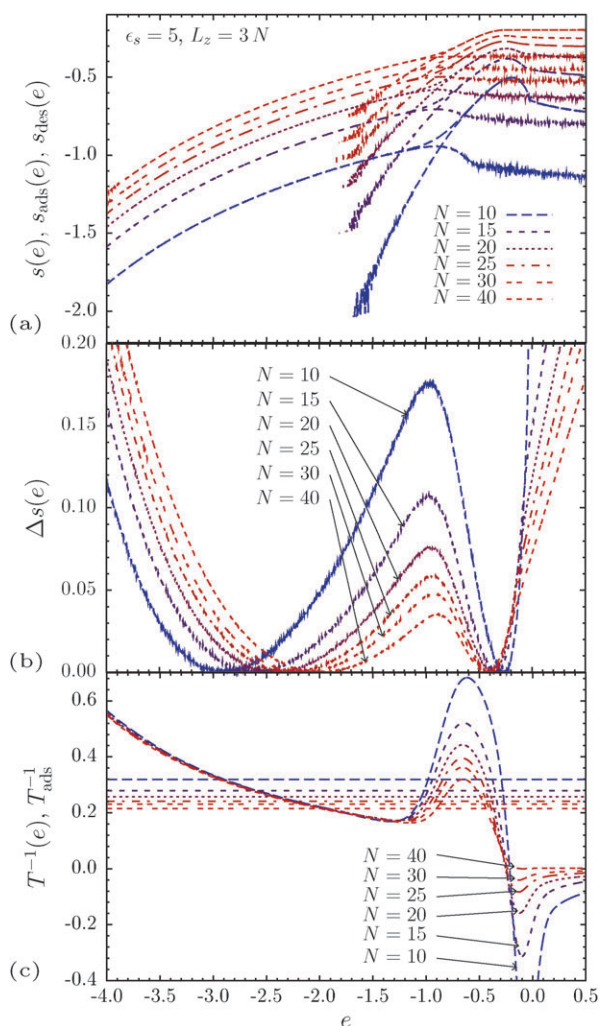
Depending on ε_s and thus on the energetic location of the crossing point, the adsorption transition appears to be *second-order-like* ($\Delta q = 0$ for $\varepsilon_s \lessgtr 2$) or *first-order-like* ($\Delta q > 0$ for $\varepsilon_s \gtrless 2$) for a finite, nongrafted chain. Referring to the phase diagram in Fig. 1, the first scenario corresponds to the docking/wetting transition from desorbed globules (DG) to adsorbed globules (AG). The $T^{-1}(e)$ curves for $\varepsilon_s = 0,1$ in Fig. 3(c) do not exhibit microcanonical signatures for a first-order-like character of the adsorption transition which occurs for $\varepsilon_s = 1$, *e.g.*, near $T_{ads} \approx 0.7$ (see Fig. 1). Noticeably, the inflection points near $T_\Theta^{-1} \approx 0.77$ ($T_\Theta \approx 1.3$) indicate the Θ-transition that separates coil-like and globular conformations in the bulk (DE/DG). It is a surprising observation that the adsorption transition becomes first-order-like at the point where it falls together with the Θ-transition ($\varepsilon_s \approx 1.8$, $T \approx 1.3$). This is signaled by the saddle point of the corresponding T^{-1} curve in Fig. 3(c).

For larger values of ε_s, phase coexistence is apparent for the transition between DE and AE2. Here, the corresponding deviations $\Delta s(e)$ from the Gibbs hulls, as plotted in Fig. 3(b), become maximal at the crossing point. The curves of the inverse microcanonical temperatures decrease [*i.e.*, T^{-1} as plotted in Fig. 3(c) increases] with increasing energy in the transition region. The temperature "bends back", *i.e.*, in the desorption process from AE2 to DE, the system is cooled while energy is increased. This is a characteristic feature of first-order-like transition behavior of a finite system (called the "backbending effect")[35] and has also been observed in numerous other systems, such as, *e.g.*, peptide aggregation.[31,32] In Fig. 3(c), the Maxwell lines T_{ads}^{-1} [the slopes of the corresponding Gibbs constructions in Fig. 3(a)] are also inserted. The adsorption temperatures T_{ads} found with this construction depend roughly linearly on the surface attraction strengths, as it has already been suggested by our formerly constructed phase diagram in ref. 30. Thus, the intersections of the Maxwell lines and the T^{-1} curves are identical with the extremal points in Fig. 3(b) and are located at the respective energies e_{ads}, e_{sep}, and e_{des}. Since the desorption energies per monomer, e_{des}, converge very quickly to a constant value $e_{des}^{\varepsilon_s \to \infty} \approx -0.35$ with increasing adhesion strength, while the adsorption energies e_{ads} still change rapidly, the latent heat per monomer, Δq, increases with ε_s. The same holds true for Δs_{surf} [*cf.* Fig. 3(b)]. Hence, both, the energetic gap between the coexisting macrostates as well as the surface-entropic barrier, increase with ε_s and trivially diverge for $\varepsilon_s \to \infty$.

3.2 Chain-length dependence

Since the adsorption transition between DE and AE2 is expected to be of second order in the thermodynamic limit,[15] first-order signatures found for the finite system must disappear for the infinitely large system $N \to \infty$. Therefore, we now investigate the chain-length dependence of the microcanonical effects. Figure 4(a) shows the microcanonical entropies $s(e)$, the adsorption entropies $s_{ads}(e)$, and the desorption entropies $s_{des}(e)$ for chain lengths $N = 10,\ldots,40$. The respective slopes of $s_{ads}(e)$ and $s_{des}(e)$ near the crossing points converge to each other with increasing chain length. Hence, the depth of the convex well is getting smaller and thus also the surface entropy decreases [Fig. 4(b)]. Interestingly, the separation energies $e_{sep} \approx -0.95$ [which corresponds to the maxima of Δs in Fig. 4(b) and approximately to the location of the intersection points of $s_{ads}(e)$ and $s_{des}(e)$ in Fig. 4(a)] do not depend noticeably on N. The desorption energies e_{des} move a little, but the adsorption energies e_{ads} shift much more rapidly towards the separation point, *i.e.*, the latent heat decreases with increasing chain length. Consequently, in Fig. 4(c), the backbending of the (reciprocal) caloric temperatures is getting weaker; the adsorption temperatures converge towards a constant. Note that the microcanonical temperature of these finitely long chains is negative in the high-energy region. This is another characteristic feature of finite systems in the microcanonical analysis and disappears with increasing chain lengths, as can be seen in Fig. 4(c).
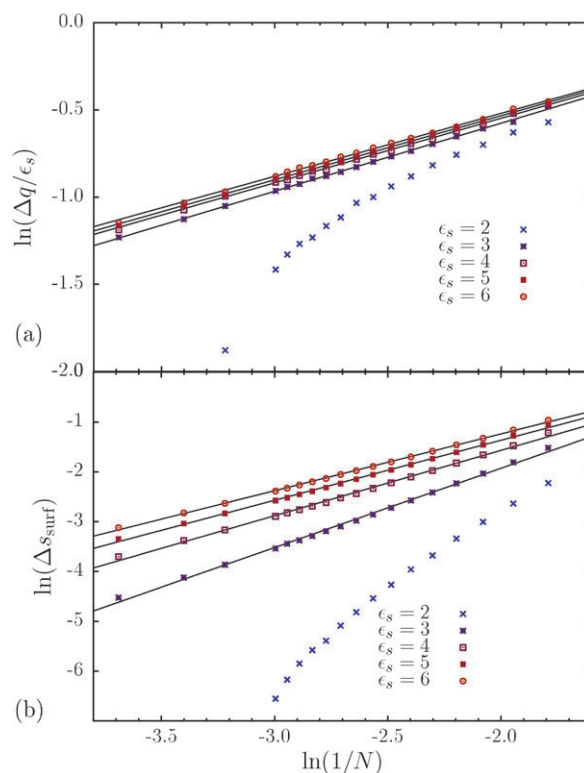
Putting all this information together, we indeed observe a clear tendency of the reduction of the microcanonical effects

Fig. 4 (a) Microcanonical entropy $s(e)$, adsorption entropy $s_{\mathrm{ads}}(e)$, and desorption entropy $s_{\mathrm{des}}(e)$ for polymers with different chain lengths $N = 10,\ldots,40$ and fixed surface attraction strength $\varepsilon_{\mathrm{s}} = 5$ in the adsorption transition regime. The maximum of $s(e)$ and the "convex intruder" begin to disappear with increasing chain length—an indication of the tendency of the adsorption transition to change its characteristics from first-order-like to second-order behavior in the thermodynamic limit; (b) deviations $\Delta s(e)$ of $s(e)$ from the Gibbs construction; (c) caloric inverse temperature curves $T^{-1}(e)$ and Maxwell lines at T_{ads}^{-1}, parametrized by chain length N.

for larger chains. The rapid decreases of latent heat and surface entropy qualitatively indicate that the adsorption transition of expanded polymers (DE to AE2) crosses over from bimodal first-order-like behavior towards a second-order phase transition in the thermodynamic limit.

In Fig. 5, the chain-length dependences of the surface entropies Δs_{surf} and of the latent heats Δq are plotted, parametrized by the surface attraction strength ε_{s}. The chains considered in our study are too short for a detailed finite-size scaling analysis. However, for $\varepsilon_{\mathrm{s}} > 2$, the plots suggest a power-law dependence of these quantities in this regime. A simple scaling *ansatz* for the surface entropy is $\Delta s_{\mathrm{surf}} \sim N^{-\kappa_s}$, while for the latent heat that trivially scales with ε_{s}, we choose $\Delta q/\varepsilon_{\mathrm{s}} \sim N^{-\kappa_q}$. The least-square fits to the data yield
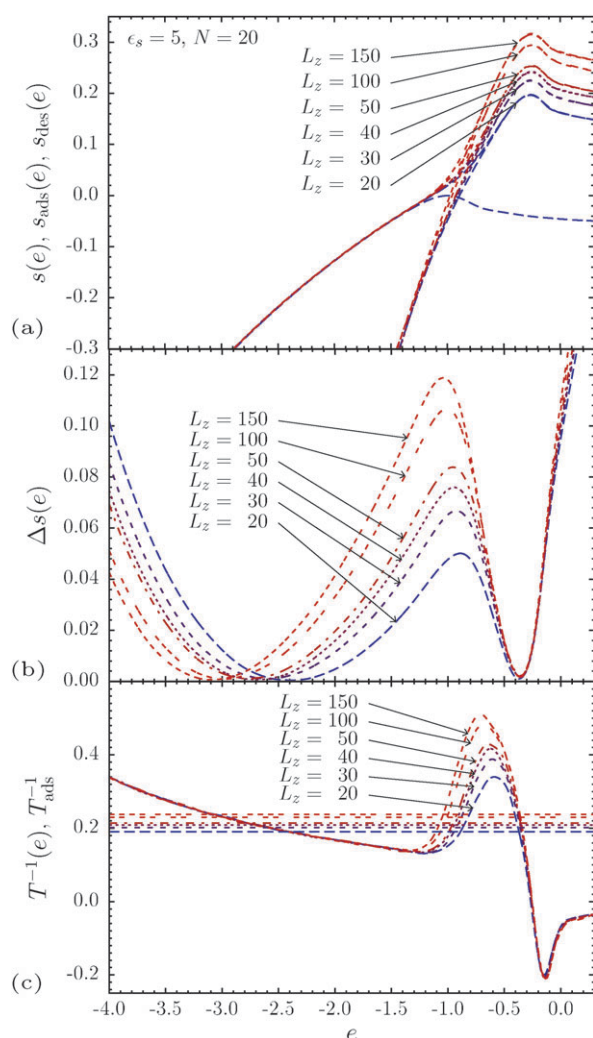

Fig. 5 Scaling with polymer length N: (a) Latent heat per monomer normalized by the surface attraction $\Delta q/\varepsilon_{\mathrm{s}}$ *vs.* inverse chain length $1/N$ for several surface attraction strengths ε_{s} and least-square fit curves to $\Delta q/\varepsilon_{\mathrm{s}} \sim N^{-\kappa_q}$. The data collapse to a single straight line for not too small ε_{s}. (b) Surface entropy per monomer Δs_{surf} *vs.* inverse chain length $1/N$ and fits to $\Delta s_{\mathrm{surf}} \sim N^{-\kappa_s}$.

$\kappa_s = 1.65(1.36,1.24,1.17)$ and $\kappa_q = 0.39(0.37,0.37,0.36)$ for $\varepsilon_{\mathrm{s}} = 3(4,5,6)$. The fit curves are also inserted into Fig. 5. The fit results for the exponents depend on ε_{s}, but seem to converge to constant positive values for $\varepsilon_{\mathrm{s}} \to \infty$. The surface entropy vanishes in the thermodynamic limit independently of the transition characteristics. However, that our data suggest $\lim_{N\to\infty} \Delta q = 0$ is support for the assumption of the second-order nature of the adsorption transition. This is consistent with results discussed in ref. 14.

3.3 Variation of the box size

Finally, after noticing that there is a considerable influence of the simulation box size on the microcanonical properties of the adsorption transition, we also want to investigate this effect in more detail. To this end, simulations with $\varepsilon_{\mathrm{s}} = 5$ for a fixed chain length ($N = 20$) were performed for different distances L_z of the steric wall to the attractive substrate. Note that fixing the chain length N, but changing L_z will also change the density. Hence, the limit of $L_z \to \infty$ considered in the following does not correspond to the thermodynamic limit. Analogously to Figs. 3 and 4, the corresponding microcanonical results are displayed in Fig. 6. Because the number of adsorbed conformations cannot depend on the amount of space available far away from the substrate, the unknown additive constants to $s(e)$, $s_{\mathrm{ads}}(e)$, and $s_{\mathrm{des}}(e)$ are chosen in such a way that $s_{\mathrm{ads}}(e)$ coincides for all L_z in Fig. 6(a). It is also possible to

11552 | *Phys. Chem. Chem. Phys.*, 2010, **12**, 11548–11554

This journal is © the Owner Societies 2010

Fig. 6 (a) Microcanonical entropies and its fractions for adsorbed and desorbed conformations, $s_{ads}(e)$ and $s_{des}(e)$, for increasing simulation box size $L_z = 20,\ldots,150$. The shape of both fractions remains unchanged for different box sizes. Only the amount of desorbed conformations increases relative to adsorbed ones for larger boxes; (b) deviations from the respective Gibbs hulls $\Delta s(e)$. An increased $s_{des}(e)$ induces an increase of the surface entropy Δs_{surf} and also slightly that of the latent heat Δq. (c) Caloric inverse temperature curves $T^{-1}(e)$ and Maxwell lines, parametrized by the distance between attractive and steric wall L_z.

overlap all $s_{des}(e)$ *via* a suitable additive constant. Hence, the *conformational* entropy does not depend on the simulation box size as long as the simulation box exceeds the chain size. This should not be surprising, since once all possible conformations can be adopted, there is nothing more to gain. All that should happen is a gain of *translational* entropy proportional to the logarithm of the simulation box size for desorbed conformations. This is exactly what the data confirm. In Fig. 6(b) the consequence of this on $\Delta s(e)$ is shown. Both, the surface entropy Δs_{surf} and the latent heat Δq increase with L_z.

It is a significant qualitative difference compared to the previous analysis of the limit $N \to \infty$ that the latent heat remains finite for large box sizes, *i.e.*, $\lim_{L_z \to \infty} \Delta q \neq 0$. Thus, the adsorption transition of the finite polymer preserves its

first-order-like character in this limit. The entropic barrier can grow arbitrarily large for large simulation boxes since the part of the phase space in proximity of the attractive substrate gets arbitrarily small. It is interesting to note here that in simulations of the grafted case no intruder was observed.

The resultant caloric inverse temperature curves $T^{-1}(e)$ in Fig. 6(c) only differ in the energy regime, where both entropic contributions, $s_{ads}(e)$ and $s_{des}(e)$, are of the same order of magnitude—the coexistence region. Once again, the effect of the intruder gets enhanced with L_z and only in this regime $T(e)$ changes with L_z. In Fig. 6(c), also the Maxwell lines representing the adsorption temperatures are shown.

One can use the knowledge of the behavior of $s_{ads}(e)$ and $s_{des}(e)$ to venture a simple estimate of T_{ads} by performing a Gibbs construction. In the adsorption phase, the contact point of the Gibbs hull is independent of L_z,

$$s(e_{ads}) = s^{trans,\|}(e_{ads}) + s^{conf}(e_{ads}), \qquad (11)$$

where $s^{trans,\|}(e_{ads})$ is the translational entropy parallel to the substrate and $s^{conf}(e_{ads})$ the conformational entropy of the adsorbed conformations. The other contact point

$$s(e_{des},L_z) = s^{trans,\perp}(e_{des},L_z) + s^{trans,\|}(e_{des}) + s^{conf}(e_{des}), \qquad (12)$$

corresponding to the entropy in the desorption phase, is a decomposition of the L_z-dependent translational entropy $s^{trans,\perp}(e_{des},L_z) = N^{-1}\ln L_z$, and the L_z-independent contributions from the translation parallel to the substrate $s^{trans,\|}(e_{des})$ and the conformational entropy $s^{conf}(e_{des})$. The adsorption temperature is obtained as the inverse slope of the Gibbs hull

$$T_{ads} = \frac{e_{des} - e_{ads}}{s(e_{des}, L_z) - s(e_{ads})}$$
$$= \frac{\Delta q}{s^{conf}(e_{des}) - s^{conf}(e_{ads}) + N^{-1}\ln L_z}. \qquad (13)$$

The conformational entropies and Δq also contain an N-dependence, but since we fixed N this is of no interest here.

For practical purposes, relation (13) allows one to restrict oneself to perform a single simulation within a sufficiently large and finite box, and one only has to keep in mind the simple $\ln(L_z)$ dependence on the simulation box size perpendicular to the substrate.

4 Summary

In our multicanonical Monte Carlo simulation study, we have investigated the adsorption transition of polymers at attractive substrates with different binding strengths by means of micro-canonical analyses. For short polymers our analysis revealed that at the adsorption transition temperature, which is here defined by a Maxwell construction, adsorbed and desorbed conformations coexist. This supports the first-order character of this transition for short polymers. The energetic separation of these conformational phases is an estimate for the latent heat which is, in principle, measurable in experiments. Thus, beside the systematic qualitative investigation of the nature of the conformational transitions, the microcanonical analysis also enables quantitative predictions.

This journal is © the Owner Societies 2010

Phys. Chem. Chem. Phys., 2010, **12**, 11548–11554 | 11553

We have studied in detail how the character of the conformational transitions depends on the surface attraction strength, chain length, and concentration. It turned out that the stronger the polymer is attracted by the substrate, the larger is the separation of the adsorption and desorption phases and the higher is the surface-entropic barrier, *i.e.*, the first-order character of the adsorption transition strengthens. This is also found if the accessible volume is increased, in which case primarily the translational entropy perpendicular to the substrate controls the surface entropy. However, if the monomer density is kept fixed, but the chain length is increased, surface entropy and latent heat vanish and the transition crosses over into a second-order phase transition in the thermodynamic limit, as expected. We performed scaling analyses for the decrease of these quantities and found them to decay slower for larger surface attraction strengths.

To conclude, our study has shown the usefulness of the microcanonical interpretation of the adsorption transition of nongrafted polymers in the regime of the polymer–substrate phase diagram[30] that is dominated by expanded conformations. This is substantial for the understanding of thermodynamic properties in deposition and self-assembly processes of short polymers or peptides at attractive substrates in good solvent. In particular, the discovery of substrate and sequence specificities in the binding of small proteins at semiconductor substrates,[8–13] with potential for nanotechnological applications, has renewed the interest in and manifested the need of a more fundamental and systematic investigation of adsorption transitions.

Acknowledgements

References

1 Y. Natsume, T. Minakata and T. Aoyagi, *Org. Electron.*, 2009, **10**, 107.
2 B. Li and N. Lambeth, *Nano Lett.*, 2008, **8**, 3563.
3 B. Geffroy, P. le Roy and C. Prat, *Polym. Int.*, 2006, **55**, 572.
4 M. A. Reed, J. Chen, A. M. Rawlett, D. W. Price and J. M. Tour, *Appl. Phys. Lett.*, 2001, **78**, 3735.
5 M. Sarikaya, C. Tamerler, A. K.-Y. Jen, K. Schulten and F. Baneyx, *Nat. Mater.*, 2003, **2**, 577.
6 J. J. Gray, *Curr. Opin. Struct. Biol.*, 2004, **14**, 110.
7 S. Brown, *Nat. Biotechnol.*, 1997, **15**, 269.
8 S. R. Whaley, D. S. English, E. L. Hu, P. F. Barbara and A. M. Belcher, *Nature*, 2000, **405**, 665.
9 R. Braun, M. Sarikaya and K. Schulten, *J. Biomater. Sci., Polym. Ed.*, 2002, **13**, 747.
10 K. Goede, P. Busch and M. Grundmann, *Nano Lett.*, 2004, **4**, 2115.
11 B. R. Peelle, E. M. Krauland, K. D. Wittrup and A. M. Belcher, *Langmuir*, 2005, **21**, 6929.
12 K. Goede, M. Grundmann, K. Holland-Nell and A. G. Beck-Sickinger, *Langmuir*, 2006, **22**, 8104.
13 M. Bachmann, K. Goede, A. G. Beck-Sickinger, M. Grundmann, A. Irbäck and W. Janke, *Angew. Chem., Int. Ed.*, 2010, in press.
14 E. Eisenriegler, K. Kremer and K. Binder, *J. Chem. Phys.*, 1982, **77**, 6296.
15 E. Eisenriegler, *Polymers near Surfaces: Conformation Properties and Relation to Critical Phenomena*, World Scientific, Singapore and New Jersey, 1993.
16 A. Milchev and K. Binder, *Macromolecules*, 1996, **29**, 343.
17 S. Metzger, M. Müller, K. Binder and J. Baschnagel, *J. Chem. Phys.*, 2003, **118**, 8489.
18 J. Krawczyk, A. L. Owczarek, T. Prellberg and A. Rechnitzer, *J. Stat. Mech.: Theory Exp.*, 2005, P05008.
19 S. Bhattacharya, V. G. Rostiashvili, A. Milchev and T. A. Vilgis, *Phys. Rev. E: Stat., Nonlinear, Soft Matter Phys.*, 2009, **79**, 030802 (R).
20 I. Gurevitch and S. Srebnik, *Chem. Phys. Lett.*, 2007, **444**, 96; I. Gurevitch and S. Srebnik, *J. Chem. Phys.*, 2008, **128**, 144901.
21 M. Lundqvist, P. Nygren, B.-H. Jonsson and K. Broo, *Angew. Chem., Int. Ed.*, 2006, **45**, 8169.
22 T. Vrbová and S. G. Whittington, *J. Phys. A: Math. Gen.*, 1996, **29**, 6253; T. Vrbová and K. Procházka, *J. Phys. A: Math. Gen.*, 1999, **32**, 5469.
23 Y. Singh, D. Giri and S. Kumar, *J. Phys. A: Math. Gen.*, 2001, **34**, L67; R. Rajesh, D. Dhar, D. Giri, S. Kumar and Y. Singh, *Phys. Rev. E: Stat., Nonlinear, Soft Matter Phys.*, 2002, **65**, 056124.
24 M. Bachmann and W. Janke, *Phys. Rev. Lett.*, 2005, **95**, 058102.
25 J. Krawczyk, A. L. Owczarek, T. Prellberg and A. Rechnitzer, *Europhys. Lett.*, 2005, **70**, 726.
26 M. Bachmann and W. Janke, *Phys. Rev. E: Stat., Nonlinear, Soft Matter Phys.*, 2006, **73**, 041802; M. Bachmann and W. Janke, *Lect. Notes Phys.*, 2008, **736**, 203.
27 J. Luettmer-Strathmann, F. Rampf, W. Paul and K. Binder, *J. Chem. Phys.*, 2008, **128**, 064903.
28 M. Bachmann and W. Janke, *Phys. Rev. E: Stat., Nonlinear, Soft Matter Phys.*, 2006, **73**, 020901 (R).
29 A. D. Swetnam and M. P. Allen, *Phys. Chem. Chem. Phys.*, 2009, **11**, 2046.
30 M. Möddel, M. Bachmann and W. Janke, *J. Phys. Chem. B*, 2009, **113**, 3314.
31 C. Junghans, M. Bachmann and W. Janke, *Phys. Rev. Lett.*, 2006, **97**, 218103; C. Junghans, M. Bachmann and W. Janke, *J. Chem. Phys.*, 2008, **128**, 085103.
32 C. Junghans, M. Bachmann and W. Janke, *Europhys. Lett.*, 2009, **87**, 40002.
33 T. Chen, X. Lin, Y. Liu and H. Liang, *Phys. Rev. E: Stat., Nonlinear, Soft Matter Phys.*, 2007, **76**, 046110.
34 J. Hernández-Rojas and J. M. Gomez Llorente, *Phys. Rev. Lett.*, 2008, **100**, 258104.
35 D. H. E. Gross, *Microcanonical Thermodynamics*, World Scientific, Singapore, 2001.
36 P. Labastie and R. L. Whetten, *Phys. Rev. Lett.*, 1990, **65**, 1567.
37 M. Schmidt, R. Kusche, T. Hippler, J. Donges, W. Kronmüller, B. von Issendorff and H. Haberland, *Phys. Rev. Lett.*, 2001, **86**, 1191.
38 D. H. E. Gross, *Rep. Prog. Phys.*, 1990, **53**, 605.
39 D. H. E. Gross, A. Ecker and X. Z. Zhang, *Ann. Physik*, 1996, **5**, 446.
40 W. Janke, *Nucl. Phys. B, Proc. Suppl.*, 1998, **63**, 631.
41 M. Kastner, M. Promberger and A. Hüller, *J. Stat. Mech.*, 2000, **99**, 1251.
42 H. Behringer and M. Pleimling, *Phys. Rev. E: Stat., Nonlinear, Soft Matter Phys.*, 2006, **74**, 011108.
43 H. Behringer, *Entropy*, 2008, **10**, 224.
44 W. Thirring, *Z. Phys.*, 1970, **235**, 339.
45 F. H. Stillinger, T. Head-Gordon and C. L. Hirshfeld, *Phys. Rev. E: Stat. Phys., Plasmas, Fluids, Relat. Interdisc. Top.*, 1993, **48**, 1469; F. H. Stillinger and T. Head-Gordon, *Phys. Rev. E: Stat. Phys., Plasmas, Fluids, Relat. Interdisc. Top.*, 1995, **52**, 2872.
46 M. Bachmann, H. Arkin and W. Janke, *Phys. Rev. E: Stat., Nonlinear, Soft Matter Phys.*, 2005, **71**, 031906.
47 W. A. Steele, *Surf. Sci.*, 1973, **36**, 317.
48 B. A. Berg and T. Neuhaus, *Phys. Lett. B*, 1991, **267**, 249; B. A. Berg and T. Neuhaus, *Phys. Rev. Lett.*, 1992, **68**, 9.
49 W. Janke, *Physica A*, 1998, **254**, 164; B. A. Berg, *Fields Inst. Commun.*, 2000, **26**, 1.
50 C. Borgs and R. Kotecký, *J. Stat. Phys.*, 1990, **61**, 79; C. Borgs and W. Janke, *Phys. Rev. Lett.*, 1992, **68**, 1738; W. Janke, *Phys. Rev. B: Condens. Matter*, 1993, **48**, 7419.
51 M. Bachmann and W. Janke, *Phys. Rev. Lett.*, 2003, **91**, 208105; M. Bachmann and W. Janke, *J. Chem. Phys.*, 2004, **120**, 6779.